Naval Research Laboratory

Washington, DC 20375-5320

NRL/MR/5675--18-9831

Measurement of UV-induced Birefringence by Thermal Annealing of a Distributed Bragg Reflector Fiber Laser

Gary A. Miller

Optical Techniques Branch
Optical Sciences Division

January 15, 2019

REPORT DOCUMENTATION PAGE

Form Approved
OMB No. 0704-0188

1. REPORT DATE *(DD-MM-YYYY)*
15-01-2018

2. REPORT TYPE
Memorandum Report

3. DATES COVERED *(From - To)*

4. TITLE AND SUBTITLE

Measurement of UV-induced Birefringence by Thermal Annealing of a Distributed Bragg Reflector Fiber Laser

5a. CONTRACT NUMBER

5b. GRANT NUMBER

5c. PROGRAM ELEMENT NUMBER
62747N

6. AUTHOR(S)

Gary A. Miller

5d. PROJECT NUMBER
UW-747-021

5e. TASK NUMBER
T051-16

5f. WORK UNIT NUMBER
6A36

7. PERFORMING ORGANIZATION NAME(S) AND ADDRESS(ES)

Naval Research Laboratory
4555 Overlook Avenue, SW
Washington, DC 20375-5344

8. PERFORMING ORGANIZATION REPORT NUMBER

NRL/MR/5675--18-9831

9. SPONSORING / MONITORING AGENCY NAME(S) AND ADDRESS(ES)

Office of Naval Research Laboratory
875 N Randolf Street
Arlington, VA 22203

10. SPONSOR / MONITOR'S ACRONYM(S)

ONR

11. SPONSOR / MONITOR'S REPORT NUMBER(S)

12. DISTRIBUTION / AVAILABILITY STATEMENT

DISTRIBUTION STATEMENT A: Approved for public release; distribution is unlimited.

13. SUPPLEMENTARY NOTES

14. ABSTRACT

The photoinduced index change of a grating in a distributed Bragg reflector (DBR) fiber laser was annealed at temper-atures up to 700 °C. In monitoring the longitudinal modes of the laser during annealing, two distinct emission bands emerged, representing the polarization dependent reflectivities of the grating being thermally processed. By fitting the emission bands to a Gaussian, a measure of the fiber's nominal (~ 7×10^{-6}) and induced (~ 5×10^{-6}) birefringence was determined.

15. SUBJECT TERMS

Fiber Bragg Grating, Fiber Laser, Thermal Annealing, Photoinduced Birefringence, Inherent Fiber Birefringence
Longitudinal Modes

16. SECURITY CLASSIFICATION OF:			17. LIMITATION OF ABSTRACT	18. NUMBER OF PAGES	19a. NAME OF RESPONSIBLE PERSON
					Gary A. Miller
a. REPORT	**b. ABSTRACT**	**c. THIS PAGE**	Unclassified Unlimited	10	**19b. TELEPHONE NUMBER** *(include area code)*
Unclassified Unlimited	Unclassified Unlimited	Unclassified Unlimited			(202) 767-9510

Standard Form 298 (Rev. 8-98)
Prescribed by ANSI Std. Z39.18

This page intentionally left blank.

CONTENTS

This page intentionally left blank.

MEASUREMENT OF UV-INDUCED BIREFRINGENCE BY THERMAL ANNEALING OF A DISTRIBUTED BRAGG REFLECTOR FIBER LASER

1. INTRODUCTION

Upon exposure to ultraviolet (UV) light, germanium-doped optical fibers undergo a positive refractive index change at near infrared (IR) wavelengths. This photoinduced index change is anisotropic with respect to the polarization eigenstates of the light traveling along the fiber and presents itself as birefringence in the effective index of the waveguide [1]. Among other effects, birefringence in fiber Bragg gratings (FBGs) manifests through a polarization dependent reflectivity (PDR) spectrum. For fiber lasers with minimal cavity birefringence, this means that two orthogonally polarized modes can experience similar cavity Q's and simultaneously lase.

It has been posited that UV-induced birefringence in optical fibers can arise when the dipole moments of defect sites in the glass matrix are aligned with the polarization of the UV writing beam [1], [2]. Radial defect sites are preferentially excited and bleached leading to an asymmetric index change [3]. Birefringence can also be caused by radial stresses formed during fabrication through structural defects that are present at the core/cladding interface [3]. Interaction between these stress fields and the polarization of light enhances the anisotropy, leading to larger index asymmetry. Axial stresses can also play a role in the index anisotropy through densification of the glass in the exposed regions of the fiber [4]. While it was proposed that a refractive index gradient across the face of the fiber generated from side exposures might cause a type of geometrical or form birefringence [5], the contribution from this effect has been shown to be minimal [2], [3], [4].

There are several techniques for measuring the photoinduced birefringence in optical fiber, though generally many of them follow the technique outlined in [1]. In this approach, carefully controlled states of polarization (SOP) are launched into the fiber and the output is characterized using a polarization analyzer. From these measurements, the Jones Matrix of a fiber section irradiated by UV light can be determined and the birefringence can be calculated. In this work, the longitudinal modes of a DBR fiber laser are used to determine the photoinduced birefringence. While the polarization eigenstates of a fiber laser are governed by the total birefringence of the laser cavity, the reflection spectra that define the laser cavity are determined by the photoinduced birefringence in the gratings. This birefringence manifests as overlapping reflection spectra separated in wavelength by an amount dependent upon the difference in effective indices of the fast and slow axes of the fiber. This principle is illustrated in Fig. 1. The laser shown here is a distributed Bragg reflector (DBR) fiber laser comprised of two, 25 mm gratings separated by a $\sim$1 m cavity (0.87 pm longitudinal mode spacing). The green lines represent the reflection spectra for polarization 1 and the red lines, polarization 2. The wavelength separation between the two sets of spectra depends on the fiber's inherent and photoinduced birefringence. When the laser is pumped, longitudinal modes aligned with one polarization axis will only reflect within the band of the grating in that axis. For gratings with reduced bandwidth (extremely long or weak), the separation between polarized longitudinal modes in these bands is more pronounced because of the limited number of modes that exist. Thus by annealing one grating in a DBR fiber

Manuscript approved January 15, 2019.

laser, two distinct emission bands will emerge, representing the PDRs of the grating being thermally processed. By measuring the wavelength separation as a function of grating strength, the fiber's birefringence can be determined.

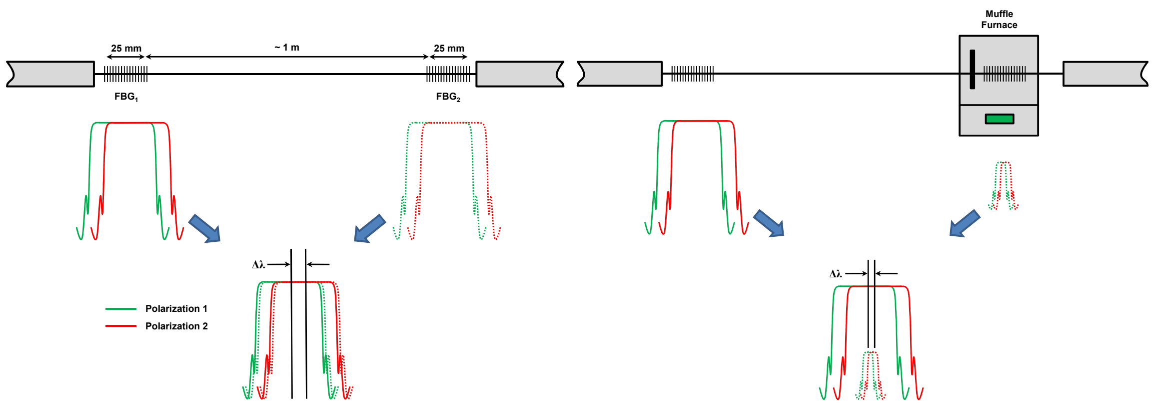

Fig. 1 — (Left) DBR fiber laser and polarization dependent reflectivities (PDRs). The arrows show the combination of the final overlapped spectra comprising the fiber laser. (Right) Setup for annealing gratings in DBR fiber lasers. The annealed grating exhibits both a reduced reflectivity and bandwidth, enabling the discrimination of PDRs.

2. EXPERIMENT

Annealing experiments were performed using a Thermolyne benchtop muffle furnace from Thermo Scientific. The DBR fiber laser was fabricated in house using a doubled argon ion laser at 244 nm to impart the refractive index change. The UV intensity at the fiber was 140 W/cm^2, and the cumulative fluence was 3 kJ/cm^2. The polarization of the UV beam was oriented perpendicular to the fiber axis to maximize the photoinduced birefringence (often referred as s-polarization). Nurfern's PS-GSF photosensitive fiber was utilized for the gratings, and PS-ESF erbium-doped fiber served as the gain medium ($\sim$75 cm). The gratings were 25 mm in length and utilized a tapered cosine apodization profile with a transition of 2.5 mm on each end. The grating strengths were 45 dB (FBG$_1$) and 41 dB (FBG$_2$).

In the experiment, FBG$_2$ was placed inside the furnace via a feedthrough port on top of the furnace. Glass wool was used to insulate the oven from the ambient air. The setup is depicted in the right diagram of Fig. 1. Next, the temperature in the oven was increased until the transmission of the FBG was reduced by 5 dB. Then, the oven was cooled to a fixed temperature (typically 100 °C) and the non-annealed grating was strain-tuned to overlap its spectrum with the annealed FBG using a piezo stage from Physik Instrumente (bottom diagrams of Fig. 1). An elevated settling temperature was necessary due to the reduction of the average induced refractive index change and subsequent blue-shift upon annealing. The transmission, reflection, and emission spectra were then taken using a high resolution optical spectrum analyzer (Apex Technologies), noting the bandwidth and reflectivity of the grating. This process was repeated until the grating was too weak to provide feedback into the cavity.

3. RESULTS

The grating at various stages of the annealing process is shown in Figure 2. Note that the spectra were adjusted for wavelength dependent insertion losses. The maximum temperature achieved was 865 °C. Using

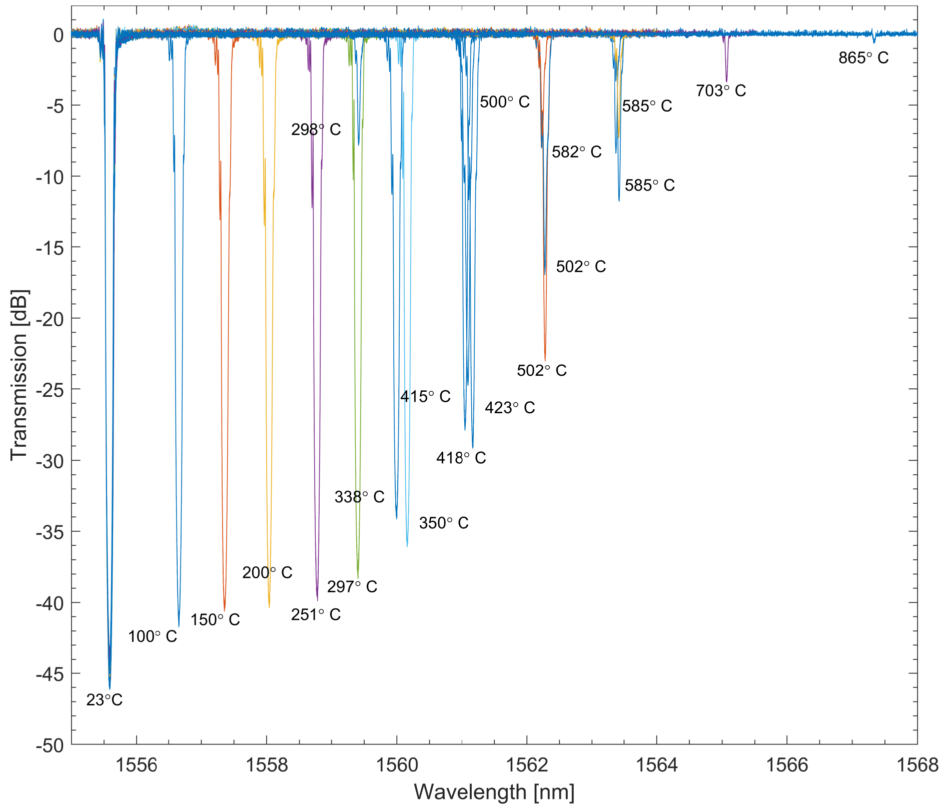

Fig. 2 — Transmission spectra of FBG_2 at various stages of thermal processing. The left most spectra is FBG_1.

the oven's internal thermocouple as a reference, the temperature-dependent wavelength shift of the fiber was 13.95 pm/°C. Figure 3 shows the transmission and emission spectra of the overlapped gratings after various annealing stages, and Table 1 lists the grating parameters for each subplot, in the order left-to-right and top-to-bottom. The peak index modulations and coupling coefficients for the grating are Δn_{mod} and κ_{peak}, respectively. The transmission values of the annealed grating ranged from 41.6 dB to 2.6 dB corresponding to an index change of 12×10^{-5} to 1.8×10^{-5}. The maximum anneal temperature was 703 °C, after which further annealing produced a grating too weak to provide feedback in the laser cavity. From the series of figures, it is apparent that as the grating strength decreases, the number of modes diminish. This decrease makes sense as annealing reduces both the bandwidth of the grating as well as the reflectivity. For lasers, the narrowed bandwidth reduces the overall spectral region longitudinal modes can exist while the lower reflectivity increases the cavity loss.

Careful scrutiny of the longitudinal modes (blue trace) in Fig. 4 reveals that the polarization modes are spectrally displaced from one another into two distinct emission bands. This is most easily seen once FBG_2 has been significantly annealed. In the plots, one polarization is denoted by green circles while the orthogonal polarization is red. As described previously, the separation is due to the PDR of the gratings and depends upon the photoinduced birefringence. The wavelength separations, induced index modulations, and resultant birefringence for the annealed spectra are listed in Table 2. The black lines in Fig. 4 represent Gaussian fits to the emission data. The wavelength separation ($\Delta\lambda$) between emission bands is found by

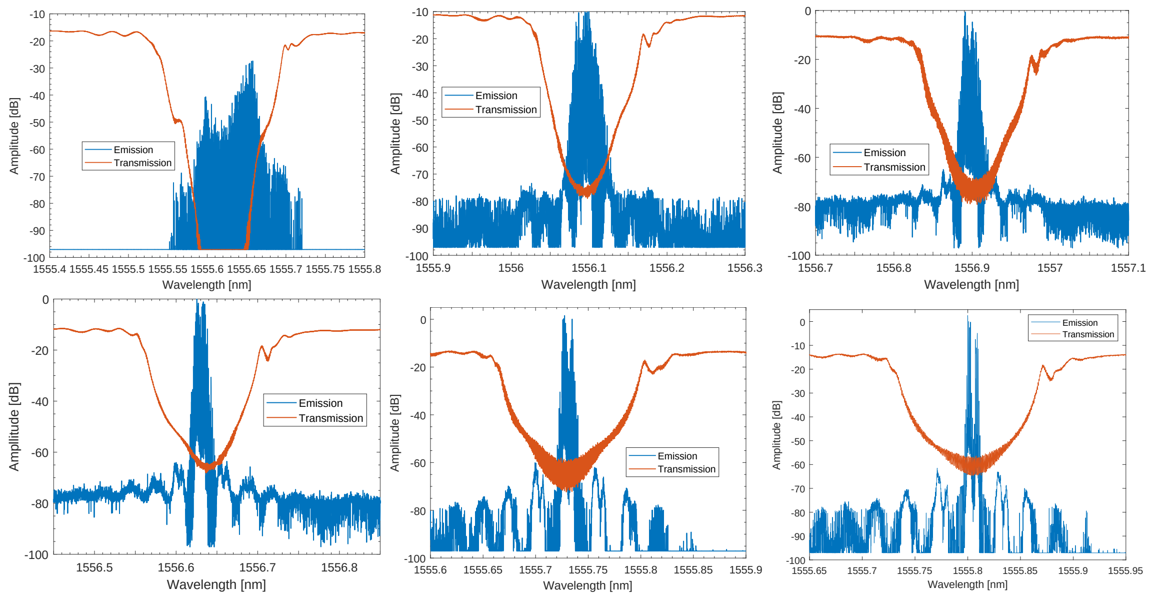

Fig. 3 — Transmission and emission spectra for the DBR fiber laser. The transmission values for FBG_2 are listed in Table 1 from left-to-right, top-to-bottom.

differencing the centers of these fits. Then, the photoinduced birefringence can be calculated using $B = \Delta\lambda/(2\Lambda)$, where Λ is the grating period (535.5 nm).

Table 1 — Grating Properties of FBG_2

Transmission [dB]	Δn_{mod} [10^{-5}]	κ_{peak} [m^{-1}]	Anneal Temperature [°C]
41.6	12.00	243.7	23
23.2	7.38	149.5	423
18.7	6.25	126.5	502
12.8	4.70	95.6	585
7.6	3.34	67.6	585
2.6	1.8	36.3	703

In the first plot of Fig. 4, the density of modes makes it challenging to separate the individual polarization modes. This is understandable considering each grating is roughly 40 dB in strength and exhibits a 3 dB bandwidth of 175 pm. The number of longitudinal modes that can exist within that bandwidth is significant (223 in this case). Additionally, the polarization modes are closely spaced due to the cavity's birefringence. An estimate of the wavelength separation can be found in this instance by examining the slope of the polarization mode fronts on the long wavelength side. Drawing a line shows a separation of roughly 13 pm, corresponding to a birefringence of 12×10^{-6}. As FBG_2 is annealed, the reflectivity decreases such that its bandwidth is well within the reflection band of FBG_1, making spectral overlap between the gratings trivial. The reduced bandwidth also helps delineate the orthogonal polarizations regardless of the cavity birefringence since the grating's spectral envelope shapes the emission bands. This can easily be

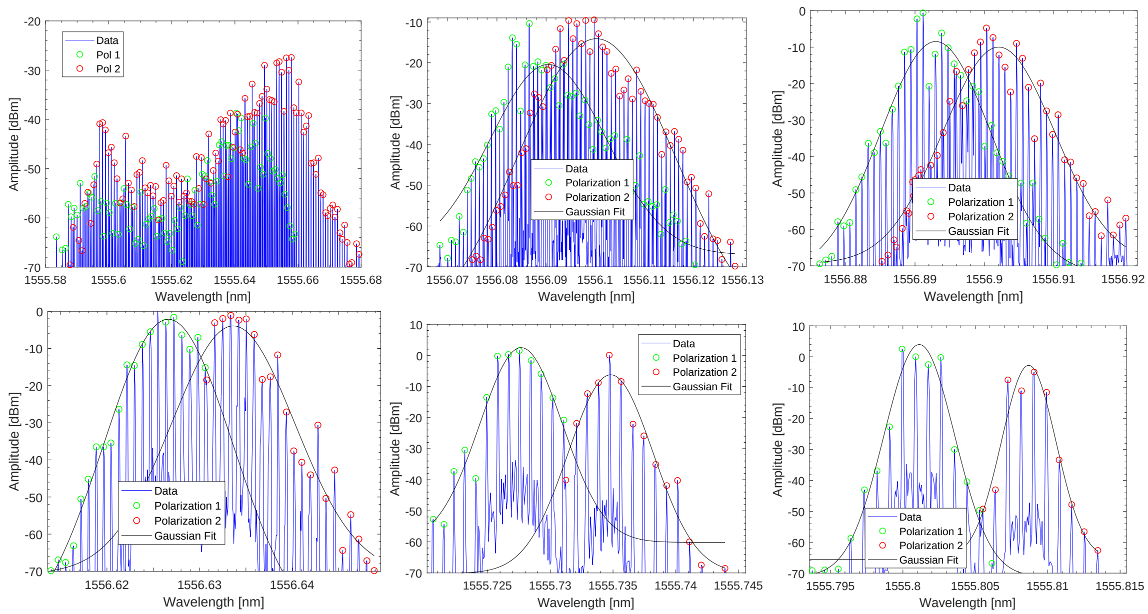

Fig. 4 — Emission spectra and Gaussian fits of the DBR fiber laser corresponding to the transmission spectra in Fig. 3. The circles designate separate polarization modes. The black curves represent Gaussian fits to the emission bands as determined by the polarization dependent reflectivities of the gratings.

Table 2 — Photoinduced Birefringence

Δn_{mod} $[10^{-5}]$	$\Delta\lambda$ [pm]	B $[10^{-6}]$
12.00	13.2	12.3
7.38	9.5	8.9
6.25	9.0	8.4
4.70	7.2	6.7
3.34	7.1	6.6
1.8	7.6	7.1

seen in the remaining plots of Fig. 4. These distinct spectral bands permit the photoinduced birefringence to be easily evaluated by noting the difference between their respective Gaussian fits.

From Table 2, approximately 1×10^{-4} refractive index modulation has been annealed, and the photoinduced birefringence has been reduced to 7×10^{-6}. Thus, thermal processing annealed approximately 5×10^{-6} of UV-induced birefringence. The estimated error in the calculation is $\pm0.42\times10^{-6}$. Figure 5 illustrates the calculated photoinduced birefringence as a function of FBG_2's index modulation. The fiber's inherent birefringence is likely on the order of 7×10^{-6}, given that the last three measurements in Table 2 are relatively constant in wavelength separation. These values agree well with measurements performed in [1], [2], [4], [5], [6], and [7].

Around an index modulation (Δn) of 4×10^{-5}, there is an abrupt change in the grating's birefringence. One possibility for this marked change could arise from the crossover of early index growth to more power law type dynamics, i.e. a shift from color center formation [8] to glass compaction [9]. This seems to correspond with research performed on early index formation in germanosilicate fibers [10] , where for high fluence exposures, the transition from one type of growth to the next occurs around 5×10^{-5}. After this threshold is reached, the birefringence continues to increase linearly with further exposure. Once again, this trend seems to correlate with previous measurements in [4], [5], [6], [7], and [11].

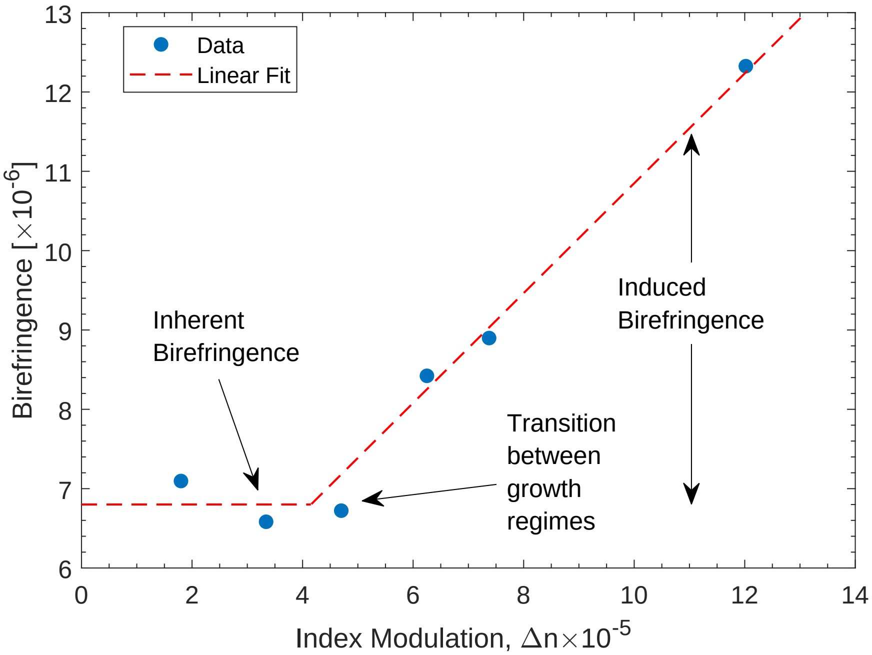

Fig. 5 — Photoinduced birefringence of FBG_2 in the heavily-doped germanium optical fiber as a function of the refractive index modulation.

4. CONCLUSIONS

The photoinduced birefringence of a highly photosensitive germanium-doped fiber was measured by monitoring the longitudinal modes of a DBR fiber laser. The birefringence was characterized by annealing one grating of the DBR in an oven and recording the laser's emission spectra. Annealing temperatures ranged from 100 °C to 865 °C. The birefringence was calculated by fitting the distinct emission bands generated from the PDR of the grating being annealed to a Gaussian and measuring the wavelength separation. The fiber's inherent birefringence was found to be 7×10^{-6}, and the UV-induced birefringence was 12×10^{-6} for an index modulation of 12×10^{-5}. The error in the birefringence calculation was estimated to be $\pm0.4\times10^{-6}$. Of note was the marked increase in photoinduced birefringence after the grating had accumulated an index change of 4×10^{-5}. This is likely due to the change in the index growth dynamics from color center formation to compaction.

ACKNOWLEDGMENTS

Funding for this project was provided by internal NRL base funding.

REFERENCES

1. T. Erdogan and V. Mizrahi, "Characterization of uv-induced birefringence in photosensitive ge-doped silica optical fibers," *J. Opt. Soc. Am. B* **11**(10), 2100–2105 (Oct 1994), doi: 10.1364/JOSAB.11.002100.

2. T. Meyer, P.-A. Nicati, P. A. Robert, D. Varelas, H.-G. Limberger, and R. P. Salathé, "Reversibility of photoinduced birefringence in ultralow-birefringence fibers," *Opt. Lett.* **21**(20), 1661–1663 (Oct 1996), doi: 10.1364/OL.21.001661.

3. J. Canning, H. J. Deyerl, H. R. Sørensen, and M. Kristensen, "Ultraviolet-induced birefringence in hydrogen-loaded optical fiber," *Journal of Applied Physics* **97**(5), 053104 (2005), doi: 10.1063/1.1856215.

4. N. Belhadj, Y. Park, S. LaRochelle, K. Dossou, and J. A. na, "Uv-induced modification of stress distribution in optical fibers and its contribution to bragg grating birefringence," *Opt. Express* **16**(12), 8727–8741 (Jun 2008), doi: 10.1364/OE.16.008727.

5. A. M. Vengsarkar, Q. Zhong, D. Inniss, W. A. Reed, P. J. Lemaire, and S. G. Kosinski, "Birefringence reduction in side-written photoinduced fiber devices by a dual-exposure method," *Opt. Lett.* **19**(16), 1260–1262 (Aug 1994), doi: 10.1364/OL.19.001260.

6. P. Lu, D. Grobnic, and S. J. Mihailov, "Characterization of the birefringence in fiber bragg gratings fabricated with an ultrafast-infrared laser," *Journal of Lightwave Technology* **25**(3), 779–786 (March 2007), doi: 10.1109/JLT.2006.889662.

7. C. Caucheteur, S. Bette, R. Garcia-Olcina, M. Wuilpart, S. Sales, J. Capmany, and P. Megret, "Influence of the grating parameters on the polarization properties of fiber bragg gratings," *Journal of Lightwave Technology* **27**(8), 1000–1010 (April 2009), doi: 10.1109/JLT.2008.2004953.

8. L. Dong, J. L. Archambault, L. Reekie, P. S. J. Russell, and D. N. Payne, "Photoinduced absorption change in germanosilicate preforms: evidence for the color-center model of photosensitivity," *Appl. Opt.* **34**(18), 3436–3440 (Jun 1995), doi: 10.1364/AO.34.003436.

9. P. Y. Fonjallaz, H. G. Limberger, R. P. Salathé, F. Cochet, and B. Leuenberger, "Tension increase correlated to refractive-index change in fibers containing uv-written bragg gratings," *Opt. Lett.* **20**(11), 1346–1348 (Jun 1995), doi: 10.1364/OL.20.001346.

10. G. A. Miller, C. G. Askins, G. A. Cranch, and E. J. Friebele, "Early index growth in germanosilicate fiber upon exposure to continuous-wave ultraviolet light," *Journal of Lightwave Technology* **25**(4), 1034–1044 (April 2007), ISSN 0733-8724, doi: 10.1109/JLT.2007.891972.

11. P. Lu, D. S. Waddy, S. J. Mihailov, and H. Ding, "Characterization of the growths of uv-induced birefringence in effective mode index and index modulation in fiber bragg gratings," *IEEE Photonics Technology Letters* **17**(11), 2337–2339 (Nov 2005), doi: 10.1109/LPT.2005.857980.